ONE IMAGE FIBRESCOPIC FRINGE PROJECTION WITH INVERSE APPROACH

Christoph Ohrt[1], Andreas Pösch[1], Dr. Markus Kästner[1], Prof. Eduard Reithmeier[1]

Institute of Measurement and Automatic Control, Leibniz Universität Hannover, Germany, christoph.ohrt@imr.uni-hannover.de

Abstract: (250 Words)

Fringe projection offers a great variety of application fields in geometry measurement of free form elements. From large measuring areas down to geometry elements with sizes in the millimeter range it can be used for fast areal measurements. With advanced deviation analyses methods errors in fabrication lines can be found promptly after their appearance which can minimize rejections. However, there are still fields that cannot be covered by classical fringe projection. One of these fields is the measurement of filigree form elements on narrow or internal carrier geometries. To overcome this drawback, a fibrescopic micro fringe projection sensor was developed [1]. The new device is capable of resolutions of less than 15 µm with uncertainties of about 35 µm in a workspace of 3x3x3 mm³.

The measuring time of the system is not sufficient for in-situ measurements, meaning measuring times of < 1 sec. The following work will introduce a new approach of applying a new one image measuring method to the fibrescopic system, based on inverse fringe projection [2]. The design of the fibrescopic fringe projection system with a laser lightsource, a digital micro-mirror device (DMD), fibre in- and uut-Coupling optics and fibre optical image bundles (FOIB) creates high demands on the on the pattern generation and the involved ray tracing simulations to adapt an exact inverse image of a given CAD model. Approaches of the simulations in the context of the complex beam path, together the drawbacks of the limited resolutions of the FOIBs shall be discussed.

Keywords: Inverse Fringe Projection, Fibrescopy, Endoscopy, Sheet Bulk Metal Forming

1. INTRODUCTION

The development of a new metal forming process demands several kinds of new technological approaches. Starting with new geometrical tool designs, fitted materials have to be found and analyzed, process parameters such as forming speeds and forces have to be optimized in respect to a maximal output at a low tool abrasion and long durability.

Concerning the new method of cold sheet bulk metal forming (SBMF) [3] that is currently developed assembly ready geometries shall be generated with a combined process of sheet and bulk forming. That means one tool in the same process step needs to bear drawing and comprehensive forces. This combination benefits early wearing effects of the SBMF-tool that may cause preterm deficient workpieces. Proper simulations for the situation can only be based on measurement data that are won from the experimental processes. To generate preferably complete datasets of the process, measurements made within the production cycle are necessary. These can only be achieved with highly accurate, fast and areal measurement devices. Experiences show that fringe projection fulfills these requirements very well [4]. However inner geometries such as SBMF-tools are not measureable in an adequate angle, which reduces the accuracy of the measurement. Common fringe projection sensors usually combine fringe generator and camera unit in a fixed housing with a predefined triangulation angle [5]. For this reason a fibrescopic fringe projection system was developed [6], that can be guided to specifically stressed areas of a SBMF-tool. These, for example, filigree side form elements suffer drawing and bulkforming forces at the same time. Early abrasion in these areas is most likely and therefor need to be taken care of at the very beginning of the development process.

In the following subchapters the principle of the fibrescopic system will be presented together with the adaption of an inverse fringe projection approach. The reduction of measurement time to a minimum in order to keep it in the range of the cycle time of the process will be explained. Methods that sufficient to realize a 100% data set after each cycle, documenting the tool abrasion at different process parameters, tool- and workpiece materials will be introduced.

2. FIBRESCOPIC FRINGE PROJECTION

2.1 Principle Setup

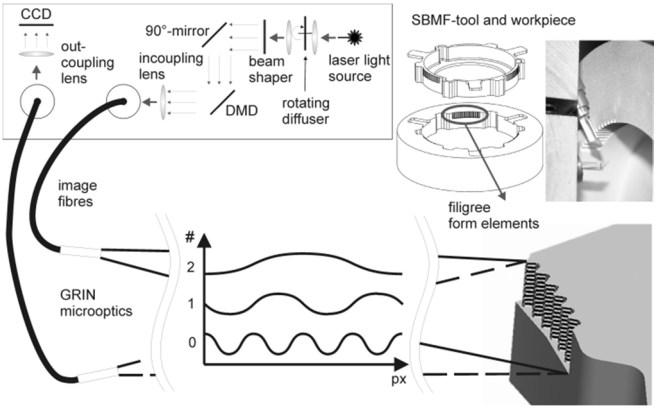

Fig. 1: Schematic of the fibrescopic fringe projection setup

Fig. 1 shows the basic design of the newly developed setup. To generate a high depth of field (DOF) with FOIBs, a good fibrecoupling at a sufficient intensity is inevitable. By their nature, laser light sources offer high intensities at a well collimated beam profile, which makes them almost ideal for

fibrecoupling. Only the coherent nature of lasers complicate the use in fringe projection since reflection on a diffuse reflecting specimen, as it is common in structured light measurements, automatically create speckle contrast, that sometime can be higher than the projected fringe pattern and thereby avoids accurate analyses [6].
To overcome this, a rotating diffusor is installed in the system together with micro lens arrays that act as beam shapers. Since the diffusor changes the speckle formation faster than the frame rate of the CCD, it leads to an integration of randomly distributed patterns which appear as a smooth light intensity image [6]. The beam shaper changes the Gaussian into a flat top distribution that is exactly fitted to the size of the DMD, that is used for the pattern generation. The pattern is focused to the 1,7 mm input aperture of the FOIB and guided 1:1 to the measurement area. The image on the specimen is projected through gradient index (GRIN) rod lenses with high NAs, that are directly attached to the FOIB.
The distorted image of the fringe pattern is recorded by a similar GRIN-FOIB arrangement in a defined triangulation angle and guided to a 5 megapixels (MP) CCD camera for computing.

2.2 Data Processing

In structured light projection sequences of a binary Gray-Code followed by cos²-phase shift pattern are dominating common of commercial fringe projection systems [4, 5]. The method shows high accuracies at a reliable robustness and therefore can be used in a wide spectrum of measurement tasks. However the projection and acquisition of the sequences take the major time of the whole measurement. Additional in fibrescopic fringe projection due to the significant loss of resolution in the 100'000 fibre image bundle, binary patterns start to fade on the cost of contrast. That complicates threshold definitions and computing. In sine or cosine patterns, threshold can be found easier, since a defined slope between maximum an minimum of a period can help finding the median. Therefore the approach of encoded phase shift [8] was adapted to the fibrescopic system. The method combines absolute phase detection with the relative accuracy of a phase shift without needing the projection of a sharp edged binary code. The procedure gets along with lesser images at a comparable accuracy and better robustness in a FOIB based system [1]. The calibration follows a black-box calibration of Zhang [9].

2.3 Resulting Data

The generated data of the specimens geometry are presented in a point cloud in cartesian coordinates. Sets of data in different geometries like plane, spheres and gearings where recorded and compared with data of other measurement systems, such as commercial fringe projection sensors and coordinate measurement machines (CMMs), as well as with original CAD design data. For the task the commercial and widely accepted software Polyworks was used. It showed that the presented system achieves accuracies of ± 10 µm for a 3D-measuremant area of 3x3x3 mm³ at standard deviations of 35 µm. This made it capable for the indicated task in SBMF.

However measuring speeds, even with the method of the encoded phase shift and the hereby reduced length of pattern sequences are not sufficient for measurements in cycle time of the SBMF process for 100% measurements of each part.

3. INVERSE FIBRESCOPIC FRINGE PROJECTION

3.1 Inverse Fringe projection

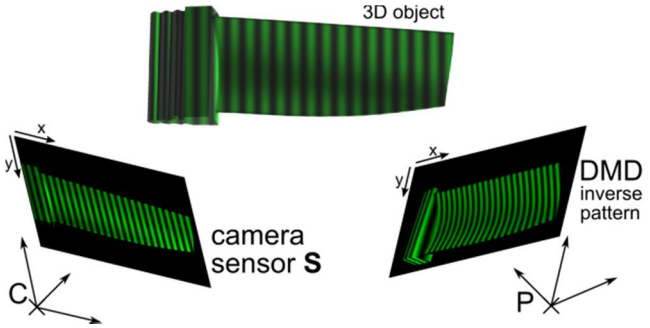

Fig. 2: Inverse fringe projection applied to a specimen

Inverse fringe projection enables measurements of 3D-geometry deviations utilizing only one special, specimen geometry adapted to an *inverse projection pattern* instead of a sequence [10]. For the inverse approach, the intended geometry needs to be known as a CAD model. The measurement setup, consisting of camera, projector and (ideal) specimen, needs to be redesigned by of ray-tracing simulations. This virtual setup must match the optical properties of the real setup; therefore a calibration procedure of the real setup must be undertaken and the parameters be considered in the ray-tracing procedure. The calibration parameters include extrinsic and intrinsic projection matrices of camera and projector as well as an estimation of lens distortions.

In the first step, the inverse projection pattern is calculated by inversion of the path of light propagation. Therefore, the camera is modeled as a projector and "emits" a straight, equidistant structured light pattern onto the specimen (CAD model); and the projector works in this context as a camera and is used to "capture" the diffuse reflection into a raster graphic with the DMD-pixels remodeled as sensor pixels. Of course, this is only possible utilizing the virtual ray-tracing-based system.

When this inverse projection pattern, obtained from the virtual system, is then projected by the real projector onto a real specimen (of the same shape and pose as the virtual specimen), the real camera will capture the beforehand-defined straight, equidistant light intensity pattern. Geometry deviations of the real specimen, however, will render distortions in the camera image which can be detected robustly using fast 2D image processing techniques. The amount of deviation of the 2D fringe pattern can be related to three dimensional geometry deviations by a linearized defect model called *sensitivity map*. Thus, quantitative information about the geometry defect is obtained. No reconstruction of point cloud data or processing of three dimensional data is required after acquisition of the measurement data allowing low latency time from measurement to result. The method is applicable e.g. to check for allowable geometry tolerances up to a µm scale.

Poesch [10] showed the prove of principle on a macroscopic fringe projector. However the optical path of a fibrescopic fringe projector as described above is far more complex to implement in ray tracing simualtions. New artifacts, such as pixelation due to the fibre bundle, have to take care of. Mainly, with the simulation of the FOIB and the in an outcoupling, but also due to the beam shaping and despeckling, new artifacts appear that may complicate the scenario.

3.2 Simulation of a fibrescopic fringe projector with raytracing

The simulation of a fibrescopic fringe projection system demands several new components in the beampath, that not only increase the complexity of the beampath, but also significantly extend the average calculation time of one complete simulative run. With the applied software FRED and a state of the art multicore computer one cycle with a sufficient number of rays needs about one hour. Since for the optimization of the several kinds of optics and the related positions numerous runs are inevitable. The setup was created component by component and connected only afterwards in one single simulation environment. First the telescope and rotating diffuser were designed for minimal divergence of the beam at a high random speckle distribution at each rotation with the given requirements mainly affecting the available space in the fringe projection sensor. For the telescope the best compromise was found with two 60 mm lenses that focus a laser with 2 mm diameter on the rotating diffuser plate. The detected rays detected behind the last lens are recorded and used as light source for the next simulation step. The flat top generator consists of the fly-eye micro lens arrays and a Fourier-Lens. The pattern that is generated by the fly-eye optics is shown on “Analyses Surface 1” in Fig. 3. The displayed section represents that the fly-eyes successfully break the wavefront of the Gaussian distribution of the laser and generate a flat top light distribution. The several maxima flatten with increasing distance to the Fourier-Lens and equalize to a homogeneous level at the stage of the DMD. The optimization criteria were a highly consistent light pattern that exactly fits to the size of the 0,7” DMD. For the DMD in the first place a fixed micro mirror array was generated that projects half of the rays to a dump and the other half to the projecting FOIB. The pattern is shown on “Analysis Surface 2” in Fig. 3. Again, the pattern is saved and used as source for the next, most computation time intensive part of the simulation. The fibre coupling part consists of an incoupling objective, that decreases the fringe image to a 1.7 mm diameter entrance of the FOIB. The fibres was simulated in the first place with 100’000 single fibre of 1 m length each. The calculation of the several hundred reflections in each fibre caused several days of simulation time. For comparison a 10 mm long version was designed. The resulting image of both fibre length after the exit was very similar, so that for simplification the 10 mm version was chosen for the rest of all simulations (Fibre coupling in Fig. 3). The specimen, using an adapted GRIN-lens that is fitted to the diameter of the FOIB. Under the triangulation angle a second GRIN-lens acquires the image in the second FOIB to a second coupling optic, that projects the resulting fringe pattern to the last analysis surface that represents the CCD of the actual setup.

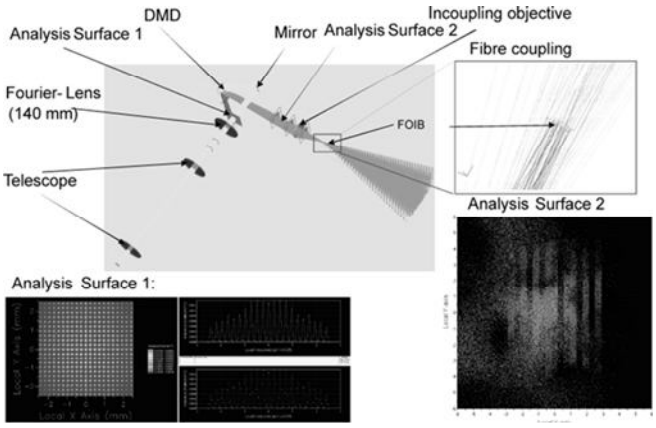

Fig. 3: Complete ray tracing design simulation of the fibrescopic fringe projection

The fringe pattern is projected, using an adapted GRIN-lens that is fitted to the diameter of the FOIB. Under the triangulation angle a second GRIN-lens acquires the image in the second FOIB to a second coupling optic, that projects the resulting fringe pattern to the last analysis surface that represents the CCD of the actual setup.

With the finished model, the behaivior of a projected pattern in the the FOIB can be predicted. Espaicially the decrease of the 1 MP image to 100’000 pixels is very uncommon for fringe projection systems as well as the availabilty of the comparatively low resultions.

Using the image of the last analayses surface the way described in chapter 3.1. enables first indications of possible qualities of an inverse fibrescopic fringe projection approach.

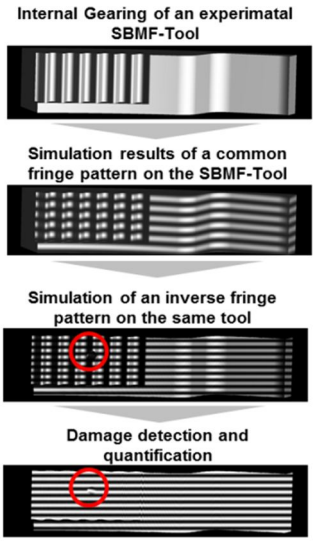

Fig. 4: Calculation results of inverse image generation with the fibrescopic fringe projection system and damage analyses on the example of the internal geometry of a SBMF-tool, following the approach of Poesch [10].

The ray tracer allows to implement a CAD-file of the desired specimen into the simulation environment. Fig. 4 shows first simulation results at a demonstrator tool of SBMF, inculding a damage detection. The damage in the two bottom images differs from the originally calculated

ideal model and therefore leads to distortion of the projected fringes.

3.3 Practical approach

For the continuous quality control of the abrasion within a SBMF-process not the CAD-model of a tool is crucial but the difference of each measurement to the one taken before. On this basis the inverse fringe pattern for each one image measurement has to be calculated from the geometry point cloud of the last measurement. Fig. 5 shows the measurement of a SBMF-deep drawing tool with the fibrescopic system. In the first step a measurement has to be taken with the common gray-code and phase shift sequence of at least 12 images. From that, with the help of the ray tracing model an inverse pattern can be generated. After finishing the next part in the production cycle the sensor head is driven back to the exact position it was placed in at the first measurement. The now projected inverse pattern, consisting of only one image, enables the fringe distortion only at sections where abrasion (either welding on, or wear off effects) has taken place. The procdure takes only several hundred of microseconds, which agrees with the beforehand made requirements. From the data an easy "out-of-tolerance" study derived, giving information about necessary tool exchanges or process stability.

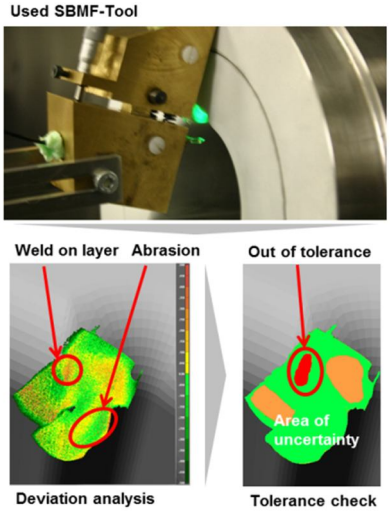

Fig. 5: Measurement of a SBMF-deep drawing tool (top) with following analyses of the point cloud in respect of abrasions effects (bottom)

Necessary accuracies in the field of SBMF are in the range of 50 to 100 µm in order to decide a tool exchange or evaluate the process parameters over a certain number of cycles.

4. DISCUSSION

The work showed that the principle of fibrescopic fringe projection works with common pattern generation approaches such as gray code and phase shift or encoded phase shift, if some compensation procedures and defined thresholds can be applied to compensate the lag of FOIB resolution. With highly collimated light sources and beam shaping a sufficient depth of focus can be achieved even with micro GRIN optics attached to the FOIBs. The working system could be transferred into a computer model for a complete ray tracing that takes account for micro optics and decrease of resolution due to the limited number of fibres in a FOIB. This is the basis for the application of virtual model based inverse fringe projection. We showed that the creation of inverse models works in principle for the fibrescopic system. We expect to achieve accuracies that are at maximum half of the accuracy of the initial fibrescopic system, which would be sufficient for the application in continuous quality control of the SBMF-process.

4. OUTLOOK

The next steps of the work on the fibrescopic fringe projection sensor will be the installation in a SBMF-machine with a highly repeatable positioning system to examine the results of the inverse fibrescopic fringe projection in reality and compare them to the simuation results.

ACKNOWLEDGEMENTS

The authors would like to thank the German Research Foundation (DFG) for funding the project B6 "Endoscopic geometry inspection" within the Collaborative Research Center (CRC) / TR 73.

REFERENCES

[1] Ohrt, C., Matthias S., Kästner, M., Reithmeier, E. : Fast endoscopic Geometry Measurement with Fiber-Based Fringe Projection for Inner Geometries, Journal of the CMSC, Vol.7, No. 2, Autumn 2012

[2] Pösch A., Vynnyk T., Kästner M., Abo-Namous O., Reithmeier E.(2010): Virtual Inverse Fringe Projection, CMSC, Reno, 2010

[3] Merklein, M.; Allwood, J. M.; Behrens, B.; Brosius, A.; Hagenah, H.; Kuzman, K.; Mori, K.; Tekkaya, E.; Weckenmann, A.: Bulk forming of sheet metal. In: Annals of the CIRP, 2(2012)61, Amsterdam: Elsevier, S. 725-745

[4] Kästner, M., 2008. Optische Geometrieprüfung präzisionsgeschmiedeter Hochleistungsbauteile. Aachen: Shaker

[5] Frankowski, G. C. M. H. T. Real-time 3D Shape Measurement with Digital Stripe Projection by Texas Instruments Micromirror Devices (DMD). Proc. of SPIE 594112-1, 2000(3958), 90–106

[6] Ohrt, C. ; Kästner, M. ; Reithmeier E. : Endoscopic geometry inspection by modular fiber optic sensors with increased depth of focus, Proc. SPIE 8082, Optical Measurement Systems for Industrial Inspection VII, 808215 (May 26, 2011); doi:10.1117/12.888921

[8] Peng, T. : Algorithms and models for 3-D shape measurement using digital fringe projections, University of Maryland, PhD-Thesis, 2007

[9] Zhang, Z. A flexible new technique for camera calibration. IEEE Transactions on Pattern Analysis and Machine Intelligence. 2000. 22(11):1330–1334

[10] Pösch A., Vynnyk, T., Reithmeier, E. : Fast detection of geometry defects on free-from surfaces using inverse fringe projection, Journal of the CMSC, Vol.8, No. 1, Spring 2013